13th International Conference on
Structural Health Monitoring of Intelligent Infrastructure
DOI: 10.3217/978-3-99161-057-1-025

Advanced Structural Monitoring and Predictive Maintenance for Railway Bridges Using Distributed Fiber-Optic Sensors

Felipe Muñoz[1,2], Iván Eguidazu[3], Julio Rodríguez[3], Diego Gaston-Beraza[1], Fernando Basarte[1], Javier Urricelqui[1], José María Pérez Casas[3], Marco Jimenez-Rodriguez[1]
[1] Uptech Sensing, Pol. Ind. Mutilva Baja, 31192 Mutilva Baja, Navarra, Spain
[2] Universidad Técnica Federico Santa María, Valparaíso, Chile
[3] SENER Mobility c\ Severo Ochoa 4, Tres Cantos. Madrid.

Email: felipe.munoz@uptech-sensing.com

ABSTRACT: This submission presents a structural monitoring solution for railway bridges and viaducts that leverages distributed fibre optic sensors (distributed temperature and strain sensing, DTSS, and distributed acoustic sensing, DAS) to capture both long-term static trends and dynamic behaviour under train loads. The long-term monitoring uses hourly DTSS strain measurements, accounting for day/night and seasonal variations, while the dynamic monitoring system records real-time strain and vibration data during train passages. By integrating these measurements with structural calculation services, the system can detect anomalies (e.g., stiffness changes, potential cracking) and inform predictive maintenance. Lastly, the results are displayed via a digital twin, providing an intuitive, web-based platform for analysing historical data and forecasting future conditions.

KEY WORDS: Distributed acoustic sensors, Distributed temperature and strain sensors, Structural health monitoring, Railway bridges.

1 INTRODUCTION

The increasing demand for reliable and efficient monitoring of critical infrastructure has driven the development and deployment of advanced sensing technologies. Among these, distributed fibre optic sensing (DFOS) has emerged as a powerful tool, offering continuous, real-time measurements over long distances with high spatial resolution [1]. Distributed temperature sensing systems (DTSS) and distributed acoustic sensing (DAS) have demonstrated significant potential in a wide range of civil engineering applications [2], [3], [4]. State-of-the-art implementations of DFOS include structural and crack monitoring, geotechnical engineering (such as landslide detection and tunnelling construction and integrity monitoring), the surveillance of buried infrastructure, and transportation infrastructure monitoring (including railways and bridges) [2]. Within this broad landscape, DAS and DTSS have been successfully applied to railway bridge monitoring, enabling early detection of structural degradation, train-induced vibrations, temperature variations, and other anomalies that could compromise safety or performance [5], [6], [7]. These implementations establish DFOS as a multi-scale monitoring solution capable of addressing both immediate safety concerns (through real-time anomaly detection) and long-term preservation needs (via historical trend analysis), while overcoming traditional limitations of discrete sensor systems through its distributed, high-resolution measurement capabilities.

In this paper, we present the results obtained from monitoring a 471-meter-long concrete viaduct used by high-speed trains. The system integrates three main units: a sensing unit, a computing unit, and an information analysis unit. The sensing unit consists of two distributed fibre optic sensors that simultaneously monitor the structure by interrogating optical fibres embedded along the structure. These sensors include a distributed acoustic sensor (DAS) and a distributed strain and temperature sensor (DTSS). The computing unit processes the measurements acquired by these sensors to calculate various structural parameters under both static and dynamic conditions. Static structural parameters are derived from measurements obtained when the viaduct is at rest, while dynamic structural parameters are obtained from measurements obtained during and after a train passage. The following static parameters are calculated: vertical displacement of the deck and displacement of the piers. Also, the calculated dynamic parameters include deck dynamic properties, vertical acceleration of the deck, bending rotation of the deck, fatigue caused at longitudinal and transverse reinforcement of the deck, and dynamic displacement of the piers. The analysis unit analyses the results to determine whether the obtained structural parameters fall within a normal range or exhibit any anomalies compared to historical data and theoretical modelling.

The structural monitoring system provides operators with two key functionalities based on temporal scope: (1) current state assessment, enabling remote evaluation of real-time structural health through comprehensive indicators and immediate risk alerts, which reduces inspection needs and optimizes maintenance responses; and (2) future state prediction, using advanced analytics to forecast structural evolution and assess capacity for future operational scenarios, thereby improving maintenance planning and infrastructure adaptability. This dual approach transforms traditional reactive maintenance into a proactive, data-driven strategy while enhancing both safety and resource efficiency.

DOI: 10.3217/978-3-99161-057-1-025

2 METHODS

Distributed fibre optic sensors

2.1.1 Distributed Temperature and Strain Sensing (DTSS)

The DTSS system employs Brillouin backscattering in optical fibres to provide continuous, high-resolution measurements of strain and temperature along the entire bridge structure. By analysing spectral shifts in the Brillouin backscattered light, DTSS achieves a spatial resolution of 0.5–1 m with strain accuracy of ±10 $\mu\varepsilon$ and temperature precision of ±0.5°C [8], [9], [10]. In this application, DTSS monitors long-term deformations and detects gradual anomalies such as settlement or bearing degradation. Its absolute strain measurement capability and high spatial resolution make it particularly suited for structural health monitoring. The optical fibre is interrogated by a UTS-FB1000 DTSS system from Uptech Sensing [11]. It is configured with 20 Hz sampling rate, a spatial resolution of 1 m, and a spatial sampling interval of 1 m, covering the full 470 m of the viaduct.

2.1.2 Distributed acoustic sensor (DAS)

The DAS system utilises phase-sensitive optical time-domain reflectometry (φ-OTDR) to detect dynamic strain variations along the optical fibre [1], [12]. Sensitive to vibrations up to several kHz, DAS captures high-frequency events including train-induced vibrations, impact loads, and sudden structural changes. In this implementation, DAS provides real-time monitoring of dynamic responses during train crossings, enabling the identification of transient phenomena. The system's dense spatial sampling allows for localised event detection across the entire bridge span. The optical fibre is interrogated by a UTS-AS1000 DAS system from Uptech Sensing [13]. It is configured with 1kHz sampling rate, a pulse width of 50 ns, a gauge length of 5 m and a spatial sampling interval of 5 m.

2.1.3 Limitations and Complementarity

While DTSS excels in static or quasi-static monitoring, its sampling rate (typically <100 Hz) [14] limits dynamic response characterisation. This limitation can be mitigated by integrating complementary information from DTSS, which provides accurate temperature measurements. By combining data from both sensors, it is possible to decouple temperature effects from true mechanical responses, enhancing the reliability of dynamic strain interpretation. Their integration in this study creates a synergistic monitoring framework: DTSS establishes baseline structural behaviour and detects slow-evolving damage, while DAS identifies transient events and verifies dynamic performance. This dual-sensor approach overcomes individual limitations, providing comprehensive structural assessment across all relevant timescales, from gradual deterioration to instantaneous dynamic loading.

Optical fibre cable installation on the structure

The monitoring system integrates DTSS and DAS interrogators within Span 1 at the viaduct's northbound section. A single optical fibre, epoxy-bonded to the structure, completes two full round trips (totalling ~2.5 km) following a systematic path: starting from the interrogators, it sequentially traverses the upper right (UR), upper left (UL), lower left (LL) and lower right (LR) surfaces. Strategic fibre loops are incorporated at deck cross-sections to capture transverse structural responses, while vertical runs instrument the piers, descending one side and ascending the opposite. This configuration achieves four complete viaduct passes, enabling comprehensive 3D monitoring through: (1) longitudinal strain profiling along all critical surfaces, (2) transverse deformation assessment via deck loops, and (3) pier behaviour characterization. Figures 1 and 2 detail the installation geometry and pier instrumentation respectively.

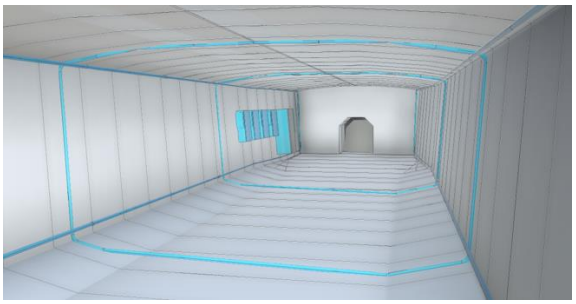

Figure 1: Optical fibre installation on a viaduct deck. Four optical fibre segments (blue lines) are installed, one on each side, as well as on the top and bottom of the deck. Additionally, loops of fibre are placed across the transverse section of the deck.

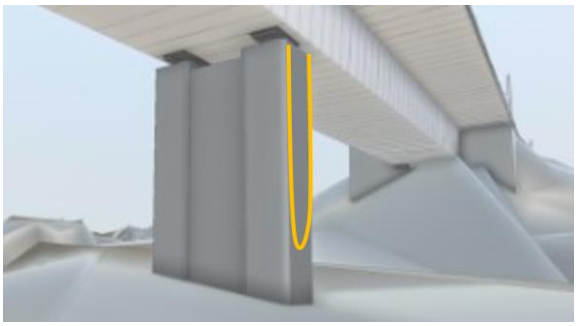

Figure 2: Optical fibre installation on the piers (orange line).

Data acquisition and processing architecture

The monitoring system utilizes both sensors in a coordinated manner to capture complementary structural responses. The DTSS sensor operates in a dual-mode configuration, performing periodic static measurements at fixed intervals to monitor long-term deformations and thermal effects, then automatically switching to dynamic-measurements mode. Simultaneously, the DAS sensor provides continuous, real-time vibration monitoring with millisecond temporal resolution, ensuring comprehensive detection of all dynamic events.

The software architecture employs modular microservices for all computational operations (characterization, alarm detection, and predictive analytics), executed through orchestrated workflows. Local processing units on the viaduct handle real-time structural characterization and immediate

DOI: 10.3217/978-3-99161-057-1-025

alarm detection, reducing data transmission volumes via 4G VPN by preprocessing sensor outputs. Cloud-based Azure services perform historical data analysis and predictive modelling, supported by: (1) a NoSQL database storing processed results in JSON format, (2) blob storage for raw sensor data archiving, and (3) a web-accessible frontend for operator interaction. Orchestrators in both environments manage service dependencies and execution sequences, ensuring proper data flow between services where outputs become subsequent inputs. This hybrid architecture optimizes bandwidth usage while maintaining complete data traceability for verification and system upgrades throughout the infrastructure's lifecycle. The data handling pipeline scheme is shown on Figure 3.

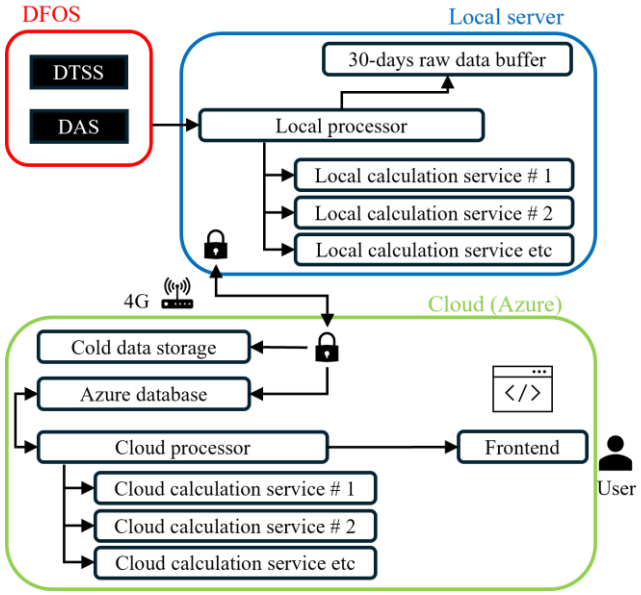

Figure 3: Data handling pipeline.

Given the dual-mode sensing architecture, accurate time synchronization is essential to correlate static (DTSS) and dynamic (DAS) measurements for event-based diagnostics and digital twin integration. Both systems independently generate data streams with embedded timestamps. To align these streams, the local processing unit performs time correlation by matching temporal features, such as strain peaks, slope reversals, or train-induced vibration signatures, across both modalities.

Time references are maintained through a hybrid synchronization approach: GPS-disciplined oscillators provide high-precision absolute timing, while NTP (Network Time Protocol) ensures fallback synchronization across distributed edge nodes and cloud-based analytics. This architecture enables sub-millisecond temporal alignment between DTSS and DAS outputs, ensuring that combined measurements reflect coherent physical events and supporting reliable fusion of static and dynamic data streams in the digital twin environment.

3 STRUCTURAL MEASURANTS AT VIADUCTS

Static measurements

At 30-minute intervals (or at a user-defined sampling rate), the system captures a ‘snapshot’ of the current deformed shape of the monitored deck and piers. Each measurement is checked to ensure displacements remain within predefined thresholds while also detecting: (1) substructure settlements, (2) bearing lockups (in instrumented piers), and (3) excessive deck deformations. This automated process enables real-time structural integrity assessment and early anomaly detection.

3.1.1 Deck’s vertical displacement

The calculation is based on the execution of four fundamental steps: (1) computation of the strains measured at the four corners of the section; (2) fitting of the curvature plane passing through these four points using a least-squares adjustment; (3) application of the generalised Mohr’s theorem in three-dimensional space to determine rotations and deflections at all points [15]; and (4) enforcement of boundary conditions at the initial point to derive displacements and rotations at any location along the deck. This systematic approach ensures accurate structural deformation analysis while accounting for geometric constraints.

Figure 4 shows the viaduct and its spans (grey background scheme) along with the static vertical displacement at all spatial locations for a specific datetime (black line). Also, historical data from 18 months (orange line indicating the historical average, while the shaded area represents the standard deviation) is shown. Analysis of the historical data reveals that each span experiences a distinct vertical displacement.

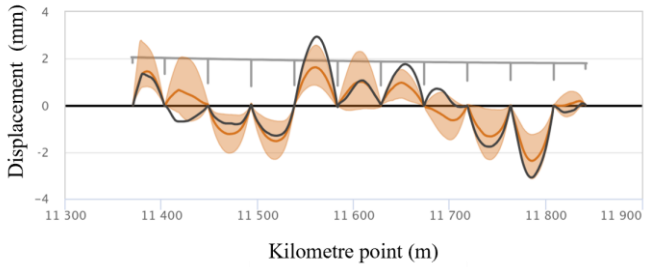

Figure 4: Deck’s static vertical displacement.

Dynamic measurements

3.2.1 Dynamic properties

This constitutes an essential service as it provides the foundation for detecting structural changes through dynamic behaviour analysis. Using the DAS measurements, the system continuously calculates the viaduct's dynamic characteristics, specifically determining for each of the first N vibration modes: (1) the natural frequency, (2) the vibrational mode shape (structural deformation pattern), and (3) the damping ratio. Using the Stochastic Subspace Identification-Covariance method (SSI-Cov) reliable operational modal analysis under ambient vibrations is performed [16]. This calculation forms the critical baseline for structural health monitoring by quantifying the bridge's dynamic fingerprint and enabling subsequent detection of behavioural deviations that may indicate damage or degradation.

DOI: 10.3217/978-3-99161-057-1-025

3.2.1.a Calculation method

The vibration characterization process involves three key stages: (1) The SSI-Cov algorithm computes vibration poles (mode shapes, natural frequencies, and damping ratios) across multiple solution orders, generating both physical and spurious results. (2) A pole stabilization stage filters non-physical poles by eliminating those with inconsistent dynamic properties (e.g., negative damping) or insufficient consensus across solution orders. (3) A final pole clustering stage, using HDBSCAN's density-based algorithm [17], groups duplicate poles from different orders while automatically determining the optimal number of clusters based on modal similarity in multidimensional space.

This robust three-stage process ensures only validated, unique vibration modes are returned, with the clustering step providing additional quality control by rejecting any remaining outliers. Figure 5 and Figure 6 shows the results of stages (1) and (3), respectively, demonstrating the algorithm's capability to distinguish physical vibration modes from computational artifacts. The implemented filtering and clustering successfully identify 20 meaningful vibration modes. Each identified vibration mode is associated to a specific mode shape which enables structural engineers to do a comprehensive analysis of the algorithm result.

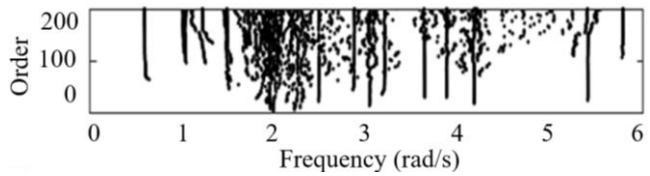

Figure 5: Vibration modes calculation at stage (1), SSI-Cov method result.

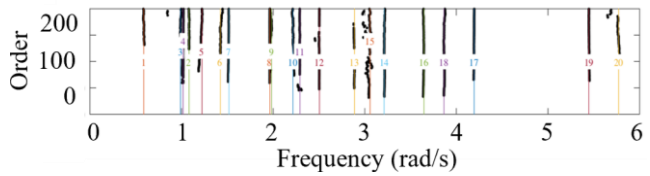

Figure 6: Identified vibration modes at stage (3) after filtering and clustering. Each mode is numbered and represented by a distinct coloured line.

3.2.1.b Dynamic behaviour change detection

This service identifies structural degradation by monitoring changes in dynamic characteristics (natural frequencies, damping ratios, and vibration modes) across multiple monitoring events, while accounting for temperature effects measured by DTSS. Using HDBSCAN clustering, it groups historically observed frequencies based on their associated mode shapes rather than simple frequency proximity. For each cluster, the algorithm: (1) quantifies temperature's influence on frequency variations, and (2) compares current frequencies against their temperature-adjusted historical interquartile ranges. When frequencies deviate beyond expected thermal-effect boundaries, the system triggers alarms indicating potential stiffness reduction (e.g., from cracking). This dual analysis of vibrational patterns and thermal compensation ensures reliable damage detection while preventing false alarms from normal temperature-induced variations.

3.2.2 Dynamic vertical displacement and bending rotation

3.2.2.a Calculation method

The dynamic analysis is initiated automatically upon detection of train passage across the structure, employing the same method used for static displacement calculations. The system acquires displacement and rotation data at each timestep, with sampling frequencies ranging from 50 Hz to 1000 Hz depending on whether DTSS or DAS sensors are utilised. For each monitored cross-section, temporal evolution analysis of the deformation data provides dynamic curvatures, dynamic rotations, instantaneous dynamic deflections, velocities (first derivatives), and accelerations (second derivatives). This methodology enables comprehensive characterisation of the structure's dynamic response under live loading conditions, while maintaining consistency with the static analysis framework through shared computational architecture.

3.2.2.b Regulatory compliance and operational limits

These parameters are strictly regulated by railway standards as they critically impact both passenger comfort and operational safety. UIC guidelines establish specific limits for dynamic structural responses, including [18]: (1) maximum permissible passenger-perceived accelerations during bridge crossings, and (2) dynamic deflection thresholds expressed as a percentage of span length - with stricter limits applying to higher train speeds. The standards define "good comfort" levels when dynamic displacements remain below these velocity-dependent thresholds. Additionally, the regulations mandate compliance with complementary safety-related limits governing structural vibrations and deformations, ensuring simultaneous satisfaction of both comfort criteria and essential safety requirements throughout the infrastructure's operational life. These parameters are used together with the historical behaviour of structural parameters to define alarms and behavioural changes.

3.2.2.b.1 Vertical dynamic displacement

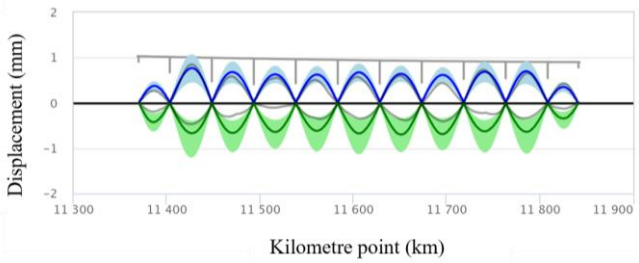

Figure 7: Deck's dynamic vertical displacement.

Figure 7 illustrates the viaduct and its piers (grey background scheme) together with the vertical dynamic displacement of the deck induced by a train passage for all spatial locations of the viaduct (grey line). Additionally, statistical values derived from

DOI: 10.3217/978-3-99161-057-1-025

18 months of operational data are presented. The blue and green lines indicate the maximum and minimum average displacement values, respectively, while the shaded areas represent the corresponding standard deviations for positive (blue) and negative (green) displacement values. This visualization enables direct comparison between instantaneous structural response and long-term performance trends, facilitating the identification of anomalous behaviour or progressive stiffness degradation.
The historical displacement monitoring results demonstrate two key structural behaviours: spans in direct contact with the ground (Spans 1 and 11) exhibit significantly reduced displacement amplitudes (0.2-0.4 mm) due to enhanced restraint from soil-structure interaction, while all spans show consistent asymmetric response with positive displacements (+0.8 mm peak) being approximately 30% smaller than negative displacements (-1.2 mm peak).
Also, the results indicate that vertical displacement is maximum at midspans and minimum at the piers, being consistent with expected behaviour for this type of structure.

3.2.2.b.2 Vertical dynamic acceleration

Deflection calculation throughout curvature integration allows the derivation of vertical accelerations of the deck, enabling to check safety and comfortability on the train. Figure 8 illustrates the vertical dynamic acceleration of the deck induced by a train passage for all spatial locations of the viaduct (grey line), together with its historical values. The blue and green lines indicate the maximum and minimum average acceleration values, respectively, while the shaded areas represent the corresponding standard deviations for positive (blue) and negative (green) acceleration values. Similar to the previous case, the historical acceleration data reveals consistent spatial trends across the viaduct: Spans 1 and 11, which interface with the ground, exhibit lower peak accelerations compared to intermediate spans. Also, the maximum acceleration occurs at the centre of the spans and minimum at the piers.

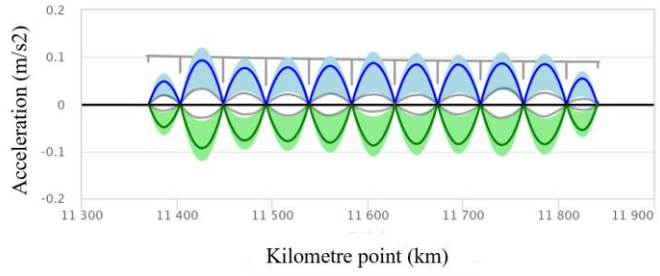

Figure 8: Deck's dynamic vertical acceleration.

3.2.2.b.3 Bending rotation

Curvature integration enhances the calculation of the induced rotations of pot bearings. Figure 9 illustrates the bending rotation induced by a train passage for all spatial locations of the viaduct (grey line), together with its historical values. The blue and green lines indicate the maximum and minimum average bending values, respectively, while the shaded areas represent the corresponding standard deviations for positive (blue) and negative (green) bending values. The historical data analysis reveals distinct rotational pattern along the viaduct, with maximum rotation occurring near the piers and minimum rotation at midspan locations. This behaviour is consistent with expected structural mechanics for simply supported spans.

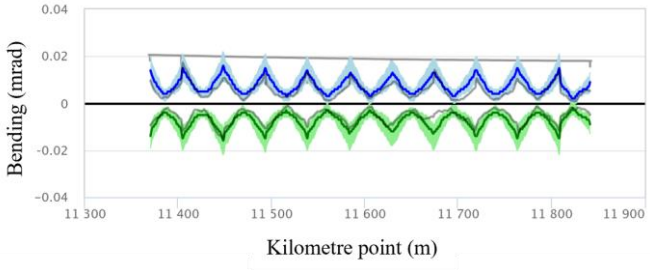

Figure 9: Deck's dynamic bending rotation.

3.2.2.b.4 Pier's dynamic displacement

The monitoring system extends its dynamic characterization methodology to instrumented piers, employing an analogous analytical process to that implemented for the deck structure. Figure 10 shows one of the piers (grey background scheme) together with its vertical dynamic displacement after a passing train (black lines), together with its statistical values. The blue and green lines indicate the maximum and minimum average height values, respectively, while the shaded areas represent the corresponding standard deviations for positive (blue) and negative (green) height values. Historical monitoring data reveals a distinct asymmetry in displacement variability, with negative displacements exhibiting greater variance than positive displacements.

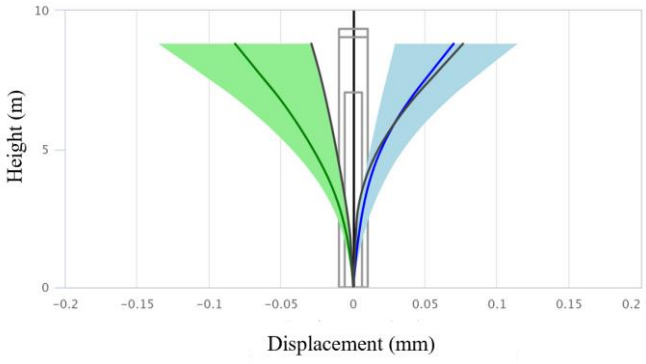

Figure 10: Pier's dynamic displacement.

3.2.3 Fatigue check of reinforcement

A major concern in railway bridges is degradation due to material fatigue, especially of steel reinforcement and prestressing [19]. Dynamic measure of the induced strain both along the deck and at specific cross sections allows to compute stress variations and fatigue cycles induced both at longitudinal prestress and transverse reinforcement [20].

DOI: 10.3217/978-3-99161-057-1-025

3.2.3.a Calculation method

Building on the dynamic strains and curvatures obtained from the previous calculation service, this module determines strain distributions across any point of the cross-section. Through extrapolation, it specifically evaluates strain conditions at reinforcement locations (which are typically more eccentric than measurement points). This enables the analysis of stress variations in both longitudinal and transverse reinforcement during each train passage.

3.2.3.b Fatigue analysis

This service analyses DTSS-measured stress data from train crossing events to quantify fatigue life consumption. The algorithm: (1) performs rainflow cycle counting to identify stress ranges and mean stresses, (2) optionally converts to equivalent alternating stress (per Eurocode EN 1992-1-1 guidelines for reinforcement/prestressing steel [21]), (3) compares results against material S-N curves to determine allowable cycles, and (4) applies Miner's rule for cumulative damage assessment [22]. Separate analyses are conducted for transverse reinforcement (from transverse fibre loops data) and longitudinal prestressing steel (from longitudinal deck fibres), with material-specific fatigue limits applied in each case.

3.2.3.c Results

Figure 11 illustrates the transverse stress distribution in the internal reinforcement (Fi) of the upper slab at section L/4 of Span 1 under different train loading scenarios. The stress profiles are evaluated for both minimum and maximum train load cases. The colour legend distinguishes the results: Min Fi is represented in green, Max Fi in gray, the average minimum stress in red, and the average maximum stress in orange. This figure highlights how internal forces respond to varying operational loads, providing insights into the structural performance of the interior reinforcement.

Figure 12 presents the transverse stress distribution in the superior reinforcement (Fs) of the upper slab at the same section under identical loading conditions. The color coding for Fs is as follows: minimum Fs is shown in red, maximum Fs in gray, the average minimum stress in green, and the average maximum stress in blue. By comparing these results with Figure 11, the figure reveals differences in stress behavior between internal and superior reinforcement layers, aiding in the assessment of load distribution and reinforcement efficiency in the slab structure.

Both figures collectively enhance the understanding of stress variations under different train loads, supporting the evaluation of structural integrity and design optimization.

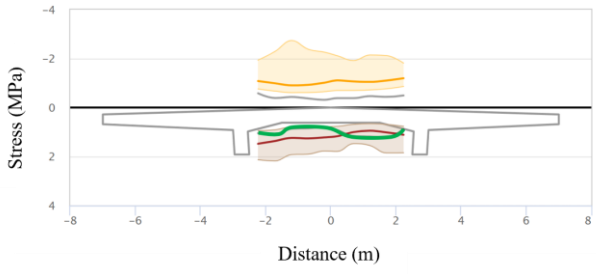

Figure 11: Deck's transverse internal reinforcement.

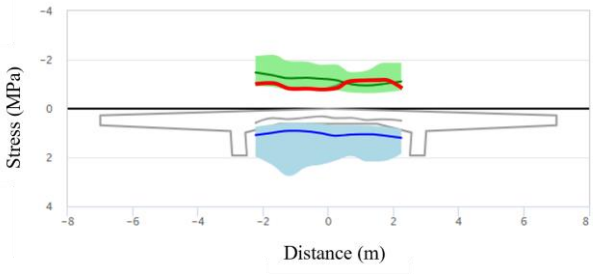

Figure 12: Deck's transverse superior reinforcement.

4 CONCLUSION

This study demonstrates the successful implementation of a dual-mode DFOS monitoring system integrating DTSS and DAS technologies for comprehensive railway bridge assessment. The system provides: (1) synchronized static-dynamic measurements (static deformations via DTSS, vibrations up to 1 kHz via DAS), (2) historical trend analysis revealing temperature-compensated structural evolution, and (3) event-based diagnostics (train responses). Results validate the approach's capability to detect stiffness changes, bearing anomalies, and fatigue-critical stress variations. The DTSS-DAS synergy establishes a new paradigm for infrastructure monitoring, combining kilometre-scale coverage with meter-resolution measurements for lifecycle management.

In addressing practical deployment aspects, the survivability of optical fibers in harsh environments, particularly under sustained dynamic loads, was considered. While tight-buffered cables were selected to minimize micro-bending losses, ongoing vibration exposure may still induce attenuation changes. Future deployments could integrate real-time loss monitoring and fiber routing strategies (e.g., loose-tube or armored cable designs) to improve durability.

Although this study focused on a 471-meter concrete viaduct, the proposed dual-mode system is adaptable to a broad range of bridge typologies, including steel truss, cable-stayed, and segmental concrete structures. For longer spans, signal processing techniques (e.g., dynamic range scaling, adaptive windowing) and distributed computing architectures can be extended to preserve performance without compromising spatial or temporal resolution.

Overall, the dual-mode DFOS platform, enhanced by edge computing, time-synchronized sensing, and AI-driven analytics, offers a robust and scalable solution for intelligent bridge monitoring across diverse operational and structural contexts.

ACKNOWLEDGMENTS

The author would like to acknowledge ADIF for lending the monitored viaduct for this project.

FUNDING

This work has been partially funded from the following projects: PTQ2021-011958 Torres Quevedo Grant from Ministerio de Ciencia, Innovación y Universidades, Government of Spain, 0011-1408-2023-000026 Doctorados Industriales of 2023 from Government of Navarra and CPP

DOI: 10.3217/978-3-99161-057-1-025

03/2021 “Soluciones tecnológicas para mantenimiento predictive de Puentes y Viaductos” from CDTI and ADIF.

REFERENCES

[1] A. H. Hartog, *An Introduction to Distributed Optical Fibre Sensors*. CRC Press, 2017. doi: 10.1201/9781315119014.

[2] M. F. Ghazali *et al.*, “State-of-The-Art application and challenges of optical fibre distributed acoustic sensing in civil engineering,” *Optical Fiber Technology*, vol. 87, Oct. 2024, doi: 10.1016/j.yofte.2024.103911.

[3] T. Wu, G. Liu, S. Fu, and F. Xing, “Recent progress of fiber-optic sensors for the structural health monitoring of civil infrastructure,” Aug. 02, 2020, *MDPI AG*. doi: 10.3390/s20164517.

[4] M. F. Bado and J. R. Casas, “A review of recent distributed optical fiber sensors applications for civil engineering structural health monitoring,” Mar. 01, 2021, *MDPI AG*. doi: 10.3390/s21051818.

[5] L. Cheng, A. Cigada, E. Zappa, M. Gilbert, and Z. Q. Lang, “Dynamic monitoring of a masonry arch rail bridge using a distributed fiber optic sensing system,” *J Civ Struct Health Monit*, vol. 14, no. 4, pp. 1075–1090, Apr. 2024, doi: 10.1007/s13349-024-00774-0.

[6] K. Kishida, T. L. Aung, and R. Lin, “Monitoring a Railway Bridge with Distributed Fiber Optic Sensing Using Specially Installed Fibers,” *Sensors*, vol. 25, no. 1, Jan. 2025, doi: 10.3390/s25010098.

[7] H. C. Su, T. H. Hsu, Y. L. Lee, W. K. Hsu, N. T. Yang, and N. H. Chang, “Fiber Monitoring System Applied to Railway Bridge Structures in a Near-Fault Region,” *Applied Sciences (Switzerland)*, vol. 14, no. 17, Sep. 2024, doi: 10.3390/app14177883.

[8] “BOTDA-Nondestructive Measurement of Single-Mode Optical Fiber Attenuation Characteristics Using Brillouin Interaction: Theory.”

[9] T. Horiguchi, K. Shimizu, T. Kurashima, M. Tateda, S. Member, and Y. Koyamada, “Development of a Distributed Sensing Technique Using Brillouin Scattering,” 1995.

[10] M. A. Soto, “Distributed Brillouin Sensing: Time-Domain Techniques,” in *Handbook of Optical Fibers*, G.-D. Peng, Ed., Singapore: Springer Singapore, 2019, pp. 1663–1753. doi: 10.1007/978-981-10-7087-7_7.

[11] Uptech Sensing, “UTS-FB1000: High-resolution Distributed Temperature and Strain sensing unit,” https://uptech-sensing.com/producto-ampliado-uts-fb1000.html.

[12] Z. He and Q. Liu, “Optical Fiber Distributed Acoustic Sensors: A Review,” Jun. 15, 2021, *Institute of Electrical and Electronics Engineers Inc.* doi: 10.1109/JLT.2021.3059771.

[13] Uptech Sensing, “UTS-AS1000: High-resolution Distributed Acoustic Sensing Unit,” https://uptech-sensing.com/producto-ampliado-uts-as1000.html.

[14] Y. Dong, “High-Performance Distributed Brillouin Optical Fiber Sensing,” Mar. 01, 2021, *Springer Verlag*. doi: 10.1007/s13320-021-0616-7.

[15] S. P. Timoshenko and J. N. Goodier, *Theory of Elasticity*, 3rd ed., vol. 144. New York: McGraw-Hill, 2018. doi: 10.1061/(ASCE)ST.1943-541X.0002064.

[16] P. Van Overschee and B. De Moor, “Subspace algorithms for the stochastic identification problem,” *Automatica*, vol. 29, no. 3, pp. 649–660, 1993, doi: https://doi.org/10.1016/0005-1098(93)90061-W.

[17] C. Malzer and M. Baum, “A Hybrid Approach To Hierarchical Density-based Cluster Selection,” Apr. 2019. doi: 10.48550/arXiv.1911.02282.

[18] International Union of Railways (UIC), “UIC Code 776-2: Design requirements for rail-bridges based on interaction phenomena between train, track, and bridge,” Jun. 2009.

[19] European Committee for Standardization, “N 1991-2: Eurocode 1: Actions on structures – Part 2: Traffic loads on bridges,” 2003.

[20] I. Bayane, A. Mankar, E. Brühwiler, and J. D. Sørensen, “Quantification of traffic and temperature effects on the fatigue safety of a reinforced-concrete bridge deck based on monitoring data,” *Eng Struct*, vol. 196, p. 109357, 2019, doi: https://doi.org/10.1016/j.engstruct.2019.109357.

[21] European Committee for Standardization, “EN 1992-1-1: Eurocode 2: Design of Concrete Structures – Part 1-1: General Rules and Rules for Buildings,” 2004.

[22] C. Ríos, J. C. Lancha, and M. Á. Vicente, “Fatigue in Structural Concrete According to the New Eurocode 2,” *Hormigón y Acero*, Mar. 2023, doi: 10.33586/hya.2023.3100.